POLITECNICO
MILANO 1863

SCUOLA DI INGEGNERIA INDUSTRIALE
E DELL'INFORMAZIONE

Executive Summary of the Thesis

# Exploiting Fermi Surface Anisotropy for Low-Dissipation Interconnects: A Study on Niobium Phosphide

Laurea Magistrale in Engineering Physics - Ingegneria Fisica

**Author:** Gianluca Mariani

**Advisor:** Prof. Giovanni Isella

**Co-advisors:** Dr. Bernd Gotsmann, Prof. Egor Babaev

**Academic year:** 2023-2024

## 1. Introduction

The demand for electricity in ICT technologies is rising sharply, constituting 8-10% of total consumption currently and potentially reaching 50% within a decade according to some forecasts [1]. To address this trend, mitigating power consumption is crucial. The focus of this thesis is on the power consumption of chips interconnects.

Interconnects play a critical role in delivering power and signals within chips. As chips have shrunk in size, so have the interconnects, leading to increased resistance due to reduced cross-sectional area and higher resistivity from greater boundary scattering. This results in higher power dissipation and signal delays. Research is exploring alternatives to copper, the material of use at the moment, to improve performance.

One promising strategy investigated in this thesis involves directional conductors [2]. This approach utilizes materials with anisotropic Fermi surfaces, aligning electron velocities along the current flow direction within interconnects to minimize momentum non-conserving boundary scattering. By reducing surface scattering, this method aims to lower energy dissipation and overall resistivity.

Niobium phosphide (NbP) was chosen for this study due to its significant mean free path (several microns), allowing for testing with microstructured devices fabricated using Focused Ion Beam (FIB) technology. Additionally, NbP exhibits an anisotropic Fermi surface and greater resistivity anisotropy compared to other tested materials like molybdenum phosphide (MoP) and tungsten phosphide (WP).

## 2. Experimental Methods

All devices were fabricated using a Focused Ion Beam (FIB), which directs a focused beam of gallium ions onto a nanometer-sized spot, selectively sputtering the crystal [3]. This precise microstructuring technique was employed in this study to extract lamellas from a single crystal of NbP and subsequently shape them into Hall bars. Additionally, the FIB was utilized to reduce the width of the Hall bars to investigate the impact of size on device resistivity.

Electrical measurements were carried out using a Dynacool cryostat by Quantum Design, capable of controlling temperatures from 1.7 K to 400 K. The cryostat includes a magnet with a maximum strength of 9 T, capable of generating both positive and negative magnetic fields. A horizontal rotator allowed sample orientation adjustments

relative to the magnetic field, and a motorized rotation stage was employed for automating angle-dependent measurements. Magnetic field measurements were exploited for studying the Fermi surface of niobium phosphide using quantum oscillations.
An external lock-in amplifier (MFLI from Zurich Instruments) was used to generate and acquire the electrical input signal. All measurements were conducted in AC mode employing a four-probe method.

## 3. Theoretical Model

To analyze the dependence of resistivity on device size, we employed a model based on the Boltzmann transport equation for thin wires, assuming diffusive boundaries and employing linear response theory to find stationary solutions [2].
The resistivity of thin wires is given by:

$$\rho\left(w,h\right) \approx \rho_0 \left[1 + \frac{g_2(\hat{j},\hat{n}_1)\tau}{g_1(\hat{j})w} + \frac{g_2(\hat{j},\hat{n}_2)\tau}{g_1(\hat{j})h}\right] \quad (1)$$

where $\rho_0$ is the bulk resistivity for infinite size, $\tau$ is the scattering time, $w$ is the width, and $h$ is the thickness of the device, assuming a rectangular cross-section. The functions $g_1(\hat{j})$ and $g_2(\hat{j},\hat{n})$ depend on the Fermi surface details and crystal orientation relative to the device. Their expressions are:

$$g_1(\hat{j}) = e^2 \sum_b \int_{BZ} \frac{g_s d^3k}{(2\pi)^3} \times \left(-f_0'\left(E_{\mathbf{k}b}\right)\right) \left(v_{\mathbf{k}b}^j\right)^2 \quad (2)$$

and

$$g_2(\hat{j},\hat{n}) = e^2 \sum_b \int_{BZ} \frac{g_s d^3k}{(2\pi)^3} \times \left(-f_0'\left(E_{\mathbf{k}b}\right)\right) \left(v_{\mathbf{k}b}^j\right)^2 \left|v_{\mathbf{k}b}^n\right| \quad (3)$$

where $b$ is the band index, $g_s$ is the spin degeneracy factor, $f_0'(E_{\mathbf{k}b})$ is the first derivative of the Fermi-Dirac distribution at energy $E_{\mathbf{k}b}$, $v_{\mathbf{k}b}^j$ is the velocity component along the transport direction $\hat{j}$, and $v_{\mathbf{k}b}^n$ is the velocity component along the normal $\hat{n}$ to the wire surface (denoted as $\hat{n}_1$ and $\hat{n}_2$ for width and thickness, respectively).
For explicit predictions, we adopted a simple model of the Fermi surface and velocity distribution of niobium phosphide, considering an ellipsoidal Fermi surface elongated along the $z$ axis by an anisotropy ratio $c$. The velocity model used is linear and anisotropic, reflecting the Weyl semimetal nature of NbP, with band dispersion described by:

$$E = \hbar v_F \sqrt{k_x^2 + k_y^2 + \frac{k_z^2}{c^2}} \quad (4)$$

where $v_F$ is the constant velocity along the $x$ and $y$ directions, and $k_x$, $k_y$, and $k_z$ represent the components of the momentum vector $\mathbf{k}$ in the $x$, $y$, and $z$ directions, respectively.
This model predicts velocities reduced by a factor $c$ along the $z$ axis:

$$\mathbf{v} = v_F \begin{bmatrix} \sin(\theta)\cos(\varphi)\hat{i} \\ \sin(\theta)\sin(\varphi)\hat{j} \\ \frac{\cos(\theta)}{c}\hat{k} \end{bmatrix} \quad (5)$$

where $\theta$ is the angle between $\mathbf{k}$ and the $z$ axis in reciprocal space, and $\varphi$ is the angle in the $x$-$y$ plane.
Substituting Equations 4 and 5 into 1, we obtain the explicit dependence of resistivity on the anisotropy ratio $c$:

$$\rho(w,h) \approx \rho_0 \left[1 + \frac{3v_F\tau}{8w} + \frac{3v_F\tau}{8h}\frac{1}{c}\right] \quad (6)$$

assuming transport along $x$, width $w$ along $y$, and thickness $h$ along $z$.
A larger $c$ reduces the increase in resistivity when $h$ is reduced. Figure 1 compares the resistivity dependence on $w$ and $h$ for various $c$ values.

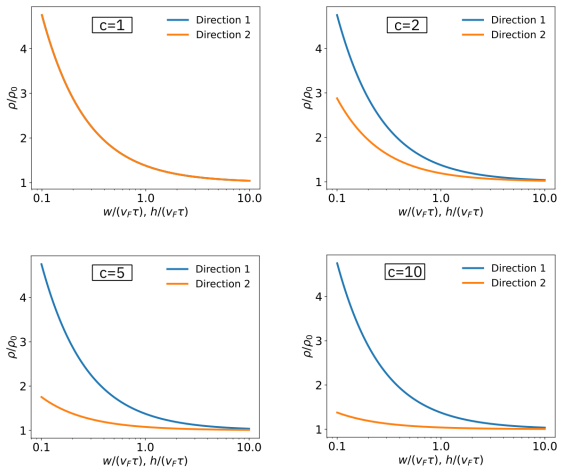


Figure 1: Resistivity dependence on width or thickness, while the other dimension is held constant.

## 4. Experimental Results

Two devices, depicted in Figure 2, were fabricated using Focused Ion Beam technology.

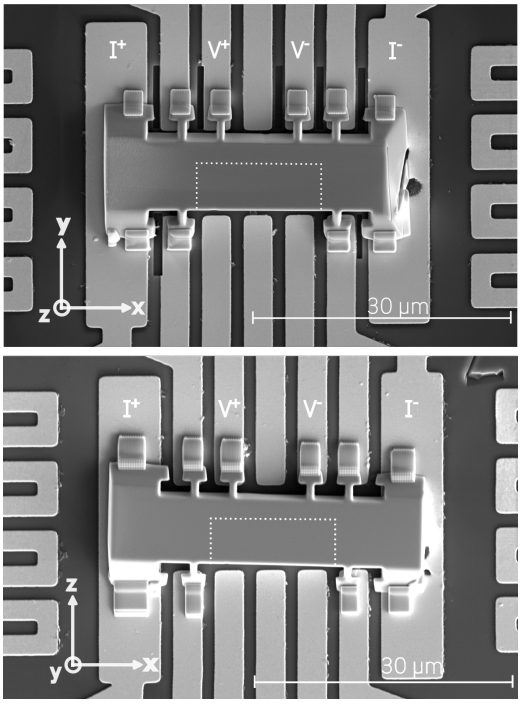


Figure 2: SEM images of Device A (top) and Device B (bottom). The axes and measurement contacts are indicated. The highlighted area denotes the region progressively reduced to study size effects on resistivity.

Device A has the $y$-axis along its width, whereas Device B has the $z$-axis aligned with its width. Based on earlier discussions, we anticipated that the resistivity of Device B would increase less rapidly than that of Device A as the width is reduced.
The experimental procedure involved systematically narrowing the width of both devices and measuring resistivity as a function of temperature at each step.
From Equations 1 and 6, the resistivity follows the relationship:

$$\rho_i(w) = \frac{A_i}{w} + B_i \tag{7}$$

where $i = 1, 2$ corresponds to the two devices. The dependence on thickness $h$ is captured in the constants $B_i$, since thickness was kept constant throughout the experiments. Equation 7 was used to fit experimental data for both devices at different temperatures, as depicted in Figure 3.

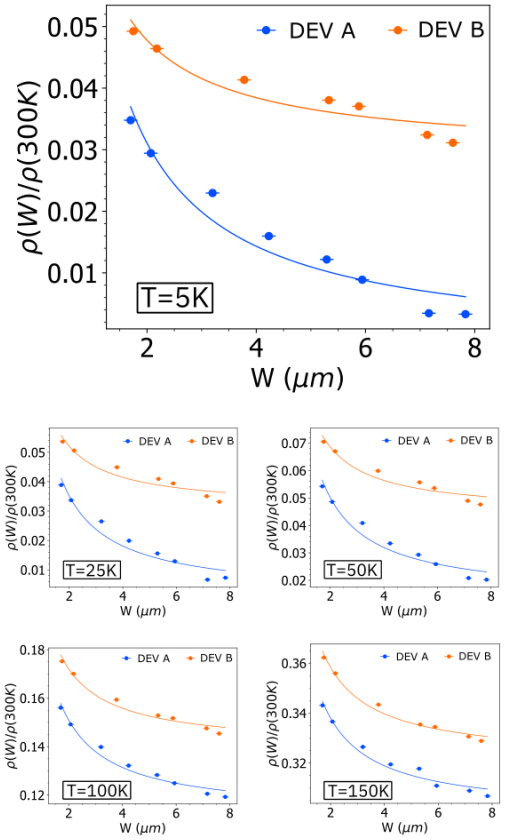


Figure 3: Resistivity versus width plots for both devices at various temperatures. Each panel shows data points fitted using Equation 7.

Due to its smaller thickness, Device B consistently exhibited higher resistivities compared to Device A.
The data shows that the increase in resistivity was slower for Device B at lower temperatures, whereas at higher temperatures the rate of increase became similar. This behavior arises because at elevated temperatures, electron mean free paths diminish, rendering them less sensitive to device boundaries.
To quantitatively compare the rate of resistivity increase between the two devices, we examined the ratio of the coefficients $A_1$ and $A_2$. This ratio provides insight into the scaling anisotropy. According to Equation 6, $c = \frac{A_1}{A_2}$. The temperature-dependent results are illustrated in Figure 4.

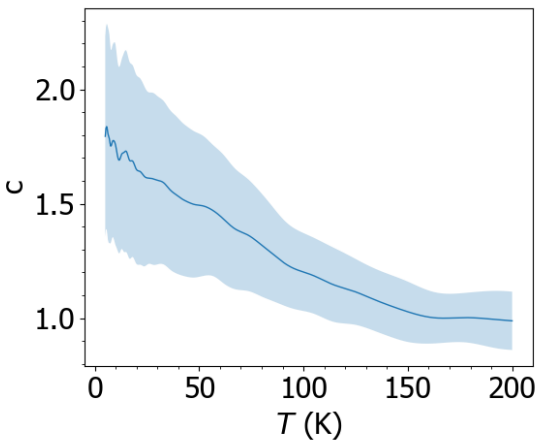


Figure 4: Anisotropy ratio $c$ as a function of temperature.

At lower temperatures, the anisotropy approaches a value close to 2, whereas at higher temperatures it converges to 1, indicative of electron mean free paths becoming significantly smaller than the device size.
These findings were corroborated by independent methods for estimating $c$, including quantum oscillations to measure Fermi surface sizes and cyclotron masses at different magnetic field orientations, as well as anisotropy in resistivity along different transport directions. The comparison of these estimates is presented in Figure 5.

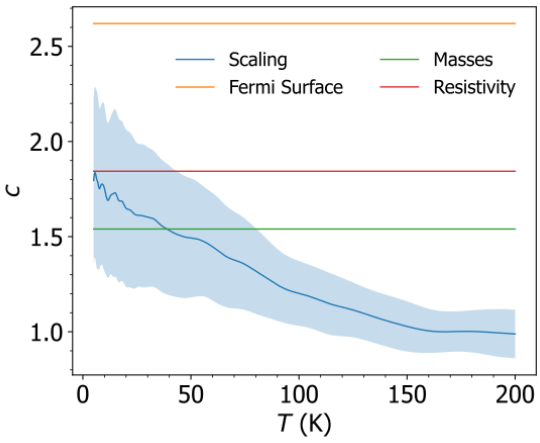


Figure 5: Comparison of anisotropy ratio $c$ estimates from different methods.

These results provide robust evidence that the anisotropy observed in scaling behavior stems from the anisotropy in the Fermi surface, thereby reinforcing the viability of directional conductors for interconnect applications.

## 5. Conclusions

The goal of this study was to demonstrate that the increase in resistivity resulting from wire size reduction can be mitigated by selecting materials with an enhanced anisotropy in the Fermi surface and by optimizing the orientation of the wires relative to the material axes.
The study revealed that resistivity of niobium phosphide increases in a distinct manner when the sample is scaled along different directions relative to the material axes. Furthermore, our findings indicated that this anisotropy becomes more pronounced at lower temperatures for this particular material.
The close agreement between anisotropy ratios derived from various transport experiments and calculations assuming an anisotropic Fermi surface provides strong evidence that the observed scaling anisotropy is indeed governed by the Fermi surface characteristics of the material.
Future research should prioritize investigating these effects at smaller length scales using materials better suited to desired specifications. Specifically, cobalt tin (CoSn) has been identified as highly promising for directional conductors at the smallest length scales [2]. These endeavors hold potential to validate a proof of concept for low-dissipation narrow interconnects, offering a viable alternative to copper in future chip scaling efforts.

## References

[1] Anders Andrae and Tomas Edler. On Global Electricity Usage of Communication Technology: Trends to 2030. *Challenges*, 6(1):117–157, April 2015.

[2] Sushant Kumar, Christian Multunas, Benjamin Defay, Daniel Gall, and Ravishankar Sundararaman. Ultralow electron-surface scattering in nanoscale metals leveraging Fermi-surface anisotropy. *Physical Review Materials*, 6(8):085002, August 2022. Publisher: American Physical Society.

[3] Philip J.W. Moll. Focused Ion Beam Microstructuring of Quantum Matter. *Annual Review of Condensed Matter Physics*, 9(1):147–162, 2018. _eprint: https://doi.org/10.1146/annurev-conmatphys-033117-054021.